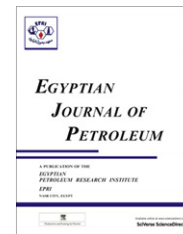




Egyptian Petroleum Research Institute
Egyptian Journal of Petroleum

www.elsevier.com/locate/egyjp
www.sciencedirect.com



Synthesis and evaluation of some new demulsifiers based on bisphenols for treating water-in-crude oil emulsions

Ahmed M. Al-Sabagh ^a, Nadia G. Kandile ^b, Rasha A. El-Ghazawy ^a,
Mahmoud R. Noor El-Din ^{a,*}

^a Egyptian Petroleum Research Institute, Nasr City, Cairo 11727, Egypt

^b Chemistry Department, Faculty of Women, Ain Shams University, Heliopolis, Cairo 11757, Egypt

Received 27 December 2010; accepted 8 March 2011

Available online 5 October 2011

KEYWORDS

Crude oil emulsions;
Demulsifiers;
Mechanism of demulsification process

Abstract The present paper endeavors to synthesize nine types of demulsifiers based on bisphenols (bisphenol A (BA), bisphenol AC (BAC) and bisphenol CH (BCH)) having different ethylene oxide units ($n = 27, 34, 45$) namely; E ($x + y$) (where E represents BA, BCH or BAC and ($x + y$) which represents the ethylene oxide units (27, 34, 45)). The chemical structures of the prepared demulsifier were elucidated using FT-IR and ¹H NMR spectra. Effect of the chemical structure (hydrophobic and ethoxylated degree of hydrophilic parts) and the mechanism of demulsification process was investigated. The data were discussed on the light of the chemical structure of the demulsifiers and the factors, effecting the demulsification process. The efficiency of these demulsifiers was tested on water-in-oil emulsions (w/o) at different concentrations (100, 200 and 300 ppm), 7.4% asphaltene content and 30%, 50% and 70% water content. From the obtained data the best demulsifier was E(34)BA which shows 100% demulsification after 58 min at 30% water content and 300 ppm of the demulsifier.

© 2011 Egyptian Petroleum Research Institute. Production and hosting by Elsevier B.V.

Open access under [CC BY-NC-ND license](#).

* Corresponding author. Tel.: +20 222745902; fax: +20 2227727433.
E-mail address: mrned04@yahoo.com (M.R. Noor El-Din).

1110-0621 © 2011 Egyptian Petroleum Research Institute. Production and hosting by Elsevier B.V. Open access under [CC BY-NC-ND license](#).

Peer review under responsibility of Egyptian Petroleum Research Institute.

doi:10.1016/j.ejpe.2011.06.008

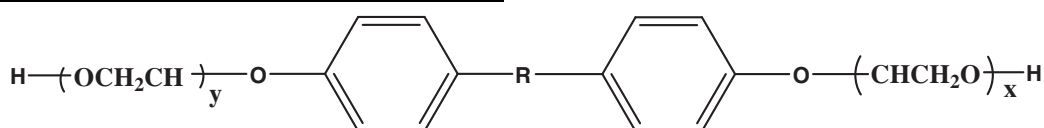


Production and hosting by Elsevier

1. Introduction

Stable water-in-oil emulsions can occur at many stages during the production and processing of crude oils [1]. The formation of these emulsions is generally caused by the presence of resins and asphaltenes, which play the role of “natural emulsifiers”, and also by wax and solids [2–5]. All these components can organize and form rigid films at the oil/water interface [6,7]. For economic and operational reasons, it is necessary to separate the water completely from the produced crude oil, the water/crude oil emulsions have to be broken (demulsified). There are various methods for crude oil demulsification, such as electro-sedimenta-

tion, supersonic demulsification, centrifugation and chemical demulsification [8]. Demulsification is an essential industrial process, mainly used for removing water and salts from crude oil. Water is dispersed as small droplets in crude oil and most of the salts are dissolved in water droplets in crude oil. If these impurities are not removed, they would cause serious corrosion and fouling in the heat exchanger and desalting equipment. To be efficient, the water content should be less than 0.5–3% after demulsification, i.e., dehydration or desalting [9]. The structure of the demulsifier can influence both of above two factors. The demulsification mechanism is quite complicated, and no demulsifier can be applied to break all kinds of crude oil emulsions [10,11]. The mechanism of demulsification and the principal role of the surfactant in destabilization of emulsion have been studied by many researchers [12]. Demulsifiers invert the gradient due to their superior surface activity, creating the film drainage phenomenon, which then leads to the coalescence of the water



droplets. The efficiency of demulsifier is determined according to the ability of the demulsifier to decrease the surface elasticity of the interfacial film [13]. It has been shown that molecules with an equal partitioning between the aqueous and the oil phase are the most efficient demulsifiers [14,15]. The conditions under which emulsion and demulsifier are contacted also affect phase separation. The present study involved preparation and characterization of demulsifiers by modification of bisphenols. The effect of demulsifiers structure, water content, demulsifier concentration, and surface tension on the efficiency of demulsifier to break water in oil emulsion was investigated.

2. Experimental

2.1. Crude oil used

An asphaltic crude oil was obtained from Gulf of Suez Petroleum Company (GUPCO, Gulf Suez, Egypt). The physicochemical properties of this crude oil are shown in Table 1.

2.2. Confirmation of chemical structure using FTIR and ^1H NMR

The Fourier Transform Infrared Spectra (FTIR) were measured on ATI Mattson–Genesis Series. The ^1H NMR were

Table 1 Physicochemical properties of the crude oil specification method results.

Specification	Methods	Results
Specific gravity at 60/60 °F	ASTM D 1298	0.874
API gravity at 60 °F	ASTM D 1298	35.29
Kinematic viscosity at 40 °C (C. St.)	ASTM D 445	14.97
Asphaltene content (wt.%)	IP 143/57	7.18
Pour point (°C)	ASTM D 97	118
Water content (vol.%)	IP 74/70	30
BS&W (vol.%)	ASTM D 4007	30.5

C. St., cent stock; API, American Petroleum Institute; BS&W, basic sediments and water contents.

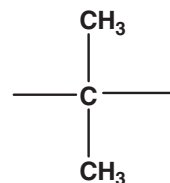
measured on Varian Genini-300 MHz spectrophotometer using DMSO as a solvent at the Egyptian Petroleum Research Institute (EPRI).

2.3. Ethoxylation of bisphenols (BA), (BAC) and (BCH)

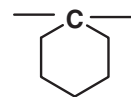
Into a (1L) two neck round bottom flask, 1 mol of bisphenol (BA, BAC or BCH) was ethoxylated using ethylene oxide gas, in presence of Na-metal (0.03 mol) as a catalyst, till the desired amount of ethylene oxide was introduced. Different ethylene oxide units were adducted namely; 27, 34 or 45 and confirmed gravimetrically. The ethoxylation reaction was carried out at 180 °C and the product was stirred at the reaction temperature for 1 h. Demulsifiers code is E(x + y) (where (x + y): represents the total ethylene oxide units (x + y) (27, 34, 45) and Y: represents BA, BCH or BAC) [16]. The chemical structure of the prepared demulsifiers is shown as follows:

where:

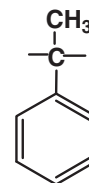
Bisphenol A: R =



Bisphenol CH: R =



Bisphenol AC: R =



$x + y = 27, 34$ or 45 ethylene oxide units.

2.4. Demulsification efficiency (bottle test)

The bottle test was used to estimate the efficiency of the demulsifiers to resolve the water-in-oil emulsions. The demulsifier in xylene was added to (100 ml) water-in-crude oil emulsion at different concentration (ppm). The mixture was stirred and was placed in a (100 ml) graduated bottle (Sani-glass) tightly

stoppered with Teflon lids. Then, the bottle was placed in a thermostatic water bath at 60 °C. Water separation (in ml) was observed every 15 min. A blank was used in each set of experiments [17].

The performance of a demulsifier was evaluated on the basis of two criteria. The first was the rate at which the water phase was released as described by the percentage of water resolution from the emulsion calculated from:

$$\text{Water resolution (vol.\%)} = (V_{\text{water}}/V_o) \times 100 \quad (1)$$

where V_{water} is the volume of separated water phase and V_o is the volume of water in the initial emulsion. The second criterion was the water concentration in the sample taken 3 cm below the surface after settling [7].

2.5. Surface tension measurements (ST)

The measurements for different concentrations of some water soluble demulsifiers were made by using platinum ring tensiometer, Kruss model at 25 °C. The instrument was daily regulated by using bi-distilled water (conductivity = $1.1 \times 10^{-6} \Omega \text{ cm}^{21}$) at 25 °C [18]. The critical micelle concentration (cmc) for the prepared surfactants was determined by the plotting of the surface tension of the surfactant solution against the logarithm of the solute concentration. The cmc values were determined from the abrupt change in the slope of plots of the surface tension versus the logarithm of the solute concentration. It must be mentioned that micelles of surfactants are formed in bulk aqueous solutions above a given concentration for each surfactant, and this concentration is known as cmc [18].

2.6. Surface tension parameters

Effectiveness of surface tension reduction (π_{cmc}): The values of the surface tension at cmc (γ_{cmc}) were used to calculate the

values of the surface pressure at cmc (γ_0) with the following equation [19,20]:

$$\pi_{\text{cmc}} = \gamma_0 - \gamma_{\text{cmc}} \quad (2)$$

where γ_0 is the surface tension measured for pure water at the appropriate temperature.

Surface excess concentration: The surface excess can be calculated with the Gibbs equation:

$$\Gamma_{\text{max}} = -10^{-7}(1/RT)(d\gamma/d\ln C)_T \quad (3)$$

where Γ_{max} is the surface excess concentration of the surfactant (mol/cm^2), R is the gas constant ($R = 8.314 \text{ J}/\text{mol K}$), T is the temperature (K), γ is the surface or interfacial tension (mN/m), and C is the concentration of the surfactant (mol/L) [21].

Minimum surface area per molecule: The average area occupied by each adsorbed molecule at the interface is given by

$$A_{\text{min}} = 10^{16}/[\Gamma_{\text{max}} \times N_A] \quad (4)$$

where A_{min} is the surface area per molecule of solute (nm^2), Γ_{max} is the surface excess concentration (mol/m^2), and N_A is the Avogadro's number [22,23].

Gibbs free energy of micellization (ΔG_{mic}): Information on the free energy of micellization was obtained indirectly from the cmc values with the following equation [24]:

$$\Delta G_{\text{mic}} = RT(1 - \alpha)Ln_{\text{cmc}} \quad (5)$$

where T is the absolute temperature and α is the fraction of counterions bound by the micelle in the case of ionic surfactants ($\alpha = 0$ for a nonionic surfactant) [25].

Gibbs free energy of adsorption (ΔG_{ads}): ΔG_{ads} was calculated with the following equation [26,27]:

$$\Delta G_{\text{ads}} = \Delta G_{\text{mic}} - (0.6022 \times \pi_{\text{cmc}} \times A_{\text{min}})$$

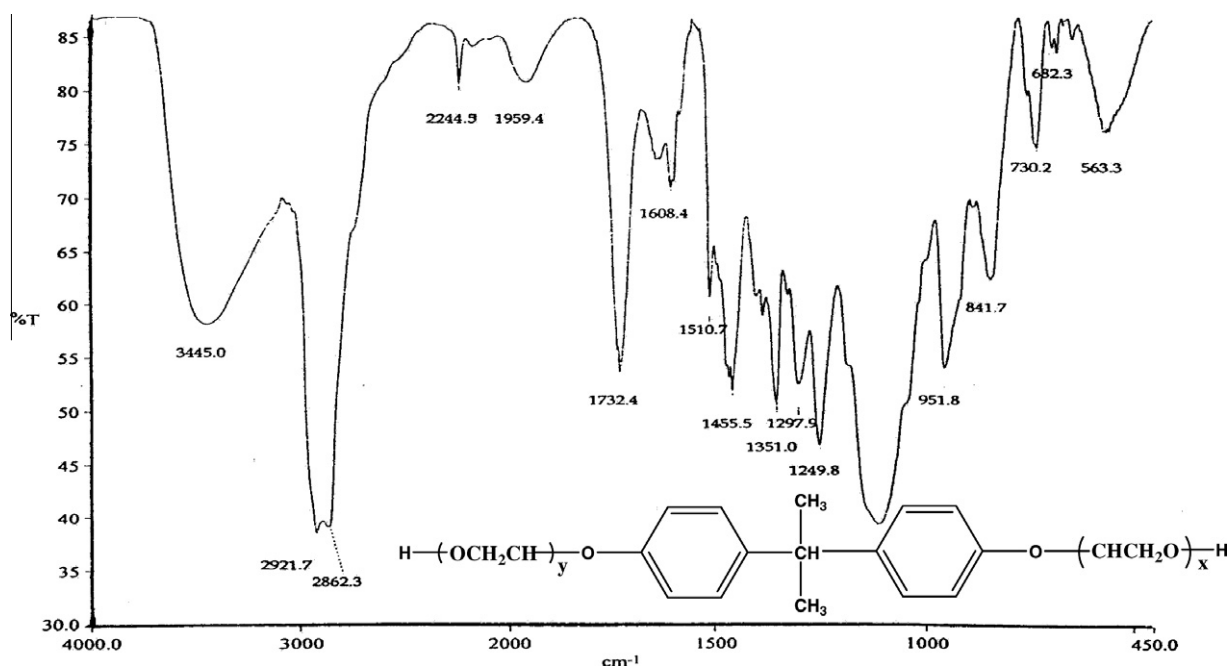


Figure 1 FT-IR spectroscopy of BA 27.

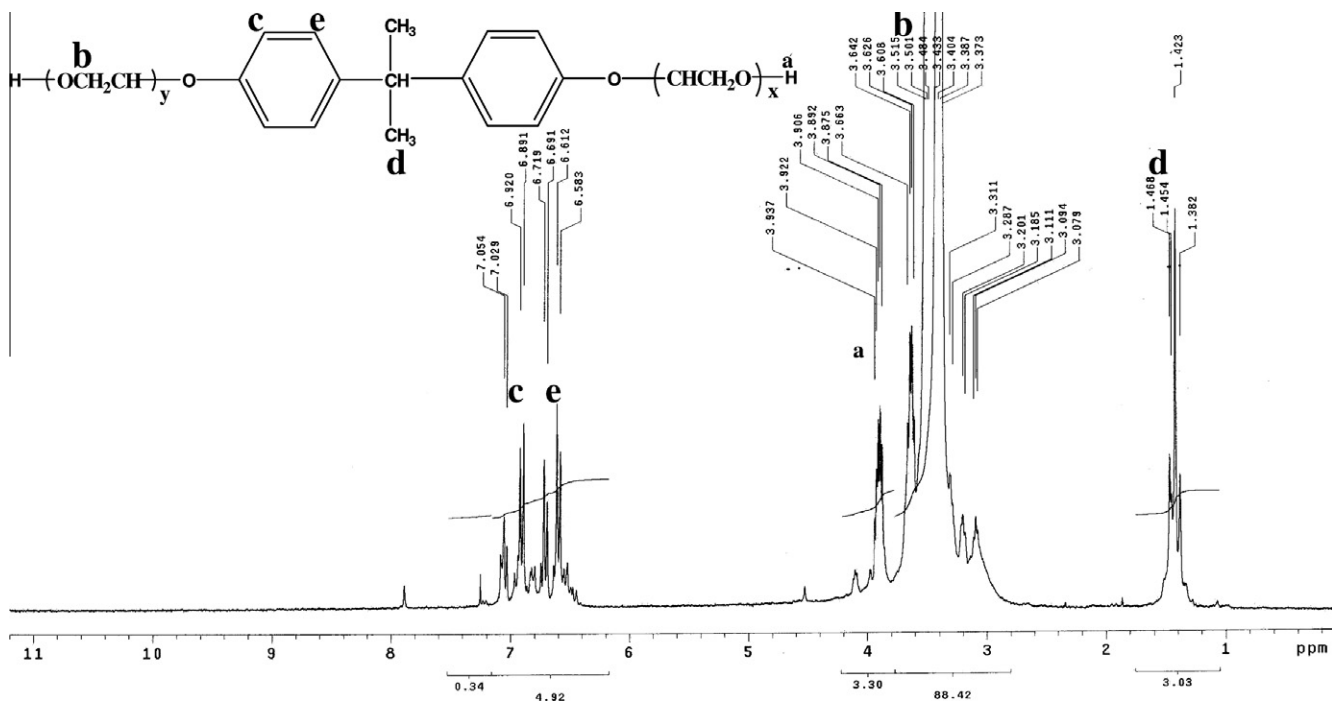


Figure 2 ^1H NMR spectroscopy of BA 27.

Table 2 Demulsification efficiency of treated and untreated crude oil emulsions (with water contents of 30%, 50% and 70%) with different concentrations for BA (27, 34 and 45) demulsifiers at 60 °C.

Demulsifier	Concentration (ppm)	Water content (%)	Time (min)	Demulsification efficiency (%)
Blank	0	30	35*	65
		50	52*	53
		70	71*	48
BA (27)	100	30	120	95
		50	109	98
		70	95	99
	200	30	100	97
		50	91	98
		70	81	99
	300	30	80	97
		50	74	98
		70	68	100
BA (34)	100	30	108	96
		50	92	96
		70	80	100
	200	30	89	95
		50	68	98
		70	67	100
	300	30	61	97
		50	50	100
		70	52	100
BA (45)	100	30	103	97
		50	89	100
		70	71	100
	200	30	79	99
		50	65	100
		70	52	100
	300	30	58	100
		50	47	100
		70	33	100

* Days instead of minutes.

Table 3 Demulsification efficiency of treated crude oil emulsions (with water contents of 30%, 50% and 70%) with different concentrations for BAC (27, 34 and 45) demulsifiers at 60 °C.

Demulsifier	Concentration (ppm)	Water content (%)	Time (min)	Demulsification efficiency (%)
BAC (27)	100	30	125	90
		50	113	95
		70	98	97
	200	30	105	95
		50	95	97
		70	84	99
	300	30	87	96
		50	77	98
		70	70	100
BAC (34)	100	30	111	94
		50	96	96
		70	84	100
	200	30	92	95
		50	81	97
		70	76	100
	300	30	73	97
		50	66	100
		70	55	100
BAC (45)	100	30	104	99
		50	92	100
		70	78	100
	200	30	82	99
		50	69	100
		70	59	100
	300	30	65	99
		50	50	100
		70	38	100

2.7. Photography and kinetic study of the demulsification process

Two demulsifiers (BA (45) and BCH (45)) were chosen for this purpose on the basis of their demulsification efficiency (low, moderate, and high, respectively). The 30% W/O emulsion was kept overnight at room temperature to get a stable emulsion without treatment. Photographic microscopy studies were carried out at 60 °C for treated and untreated emulsions. The treated and untreated emulsion samples were taken at different times with a Teflon stick for analysis. An emulsion droplet was spread on a glass slide and covered with a Teflon layer. The slides were photographed under an Olympus binocular microscope (Germany) with a camera, and the droplets were counted with the help of a Digitat 5050-R (Germany) [28].

3. Results and discussion

3.1. Confirmation of the chemical structure of BA 27 demulsifier

The FTIR spectrum of ethoxylated bisphenol A (BA 27), showed the appearance of characteristic bands at 3440 cm^{-1} for (–OH) of ethylene oxide chain (PEO) terminal, 3145 cm^{-1} for the aromatic C–H stretching of phenyl ring, 2959 and 2855 cm^{-1} for asymmetric and symmetric the aliphatic C–H stretching, 1609 and 1455 cm^{-1} pair for C=C phenyl ring stretching, 1118 cm^{-1} for C–O etheryl bonds in PEO and 835 cm^{-1} for para-substituted phenyl ring (see Fig. 1).

The ^1H NMR spectrum of ethoxylated bisphenol showed splitting at chemical shift at $\delta = 7.05\text{--}6.58$ (m, 8H, 2 Ar–H), $\delta = 3.2\text{--}3.06$ (s, 2H, CH=CH), $\delta = 3.98\text{--}3.92$ (s, 2H, CH₂), $\delta = 3.75\text{--}3.07$ (s, 4H, CH₂), $\delta = 1.45\text{--}1.40$ (s, 2H, CH₂), $\delta = 1.36\text{--}1.06$ {(s, nH, (CH₂)_n} and $\delta = 0.99\text{--}0.64$ (s, 6H, 2CH₂) (see Fig. 2).

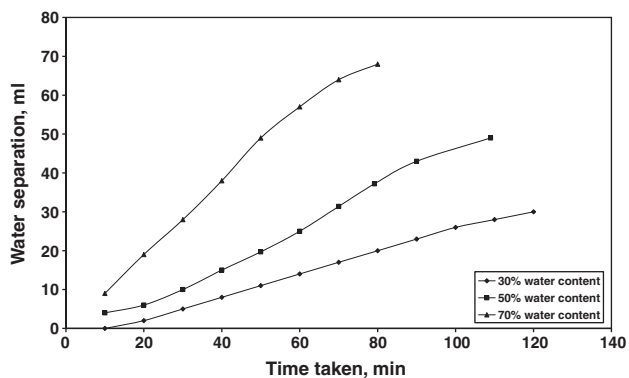
3.2. Factors affecting the demulsification efficiency

3.2.1. Water content

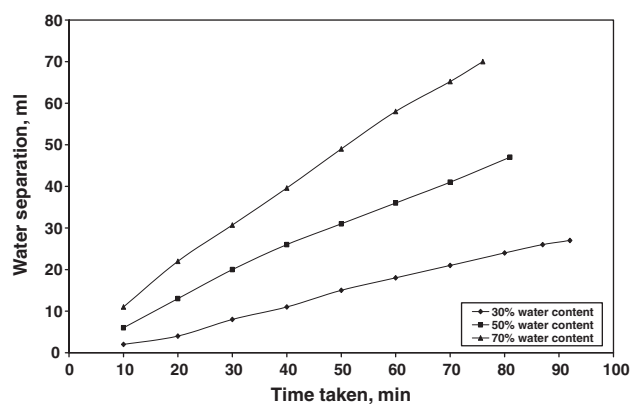
Water content in w/o emulsion is one of the important factors affecting the demulsification efficiency or the stability of an emulsion in general. The tough emulsions are not only depending on asphaltene, resin and paraffin but also on water content [29]. From the data in Tables 2–4 and the illustrations in Figs. 3–5, it is clear that the demulsification efficiency increases with increasing water content from 30% to 70% for all the investigated demulsifiers. The volume fraction of water separation is plotted versus the time taken for the different water contents in crude oil emulsions. These results indicate that the time taken for water separation and required demulsifier doses were generally decreased with increasing the water content for all demulsifiers. For example, the highly effective demulsifier (BA 45) exhibited 100% demulsification efficiency after 58, 47 and 33 min with 30%, 50% and 70% water contents, respectively at 300 ppm. On the other hand, the performance of (BCH 27) demulsifier is obtained at 130, 119 and 100 min with 30%, 50% and 70% water contents, respectively at 100 ppm. This

Table 4 Demulsification efficiency of treated crude oil emulsions (with water contents of 30%, 50% and 70%) with different concentrations for BCH (27, 34 and 45) demulsifiers at 60 °C.

Demulsifier	Concentration (ppm)	Water content (%)	Time (min)	Demulsification efficiency (%)
BCH (27)	100	30	130	88
		50	119	93
		70	100	97
	200	30	110	92
		50	98	95
		70	86	98
	300	30	91	94
		50	79	96
		70	74	98
BCH (34)	100	30	116	92
		50	100	94
		70	89	99
	200	30	100	94
		50	89	95
		70	79	98
	300	30	84	94
		50	69	97
		70	60	99
BCH (45)	100	30	110	95
		50	95	98
		70	84	100
	200	30	89	99
		50	71	99
		70	62	99
	300	30	71	99
		50	60	99
		70	45	100

**Figure 3** Effect of the water content on the demulsification efficiency of BA (27) demulsifiers at 100 ppm and 60 °C.

may be attributed to the water content in the W/O emulsion because the repulsion of the W/O interface depends on the pressure of both the internal (water) and external (oil) phases, so that at a low water content, the internal pressure of a water droplet is lower than the external pressure of an oil droplet [16]. This leads to an increase in the mechanical stability of the W/O interface and rigidity of the film. On the other hand, the rigidity of W/O films decreases with increasing water content in the bulk until the internal pressure becomes greater than the external pressure. At that moment, a rapid rupture of the W/O interface occurs, and the coalescence of water droplets increases [29].

**Figure 4** Effect of the water content on the demulsification efficiency of BAC (34) demulsifiers at 200 ppm and 60 °C.

3.2.2. Effect of demulsifier concentration

One of the most important parameters governing the adsorption of demulsifiers at the interface is the demulsifier concentration [26]. The effects of nine demulsifiers E(X) (E represented to BA, BAC and BCH and X represented to ethylene oxide unit (27, 34 and 45)) on the dewatering percentage are shown in Tables 2–4 and Figs. 6–8. The water separation accelerates with an increase in the demulsifier concentration. These data indicate that increasing the demulsifier concentration leads to an increase in the adsorption of the demulsifier molecules on the

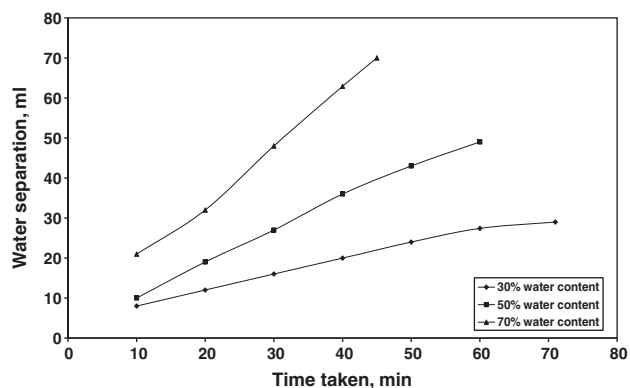


Figure 5 Effect of the water content on the demulsification efficiency of BCH (45) demulsifiers at 300 ppm and 60 °C.

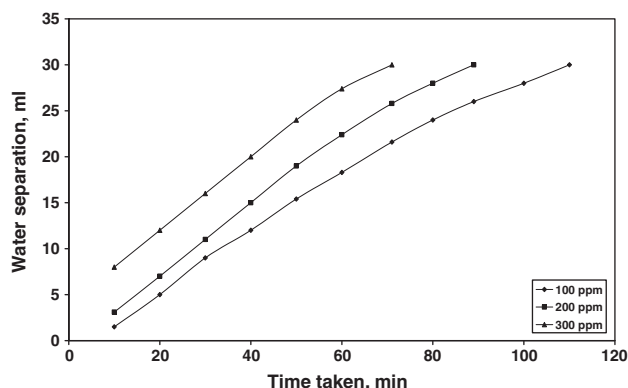


Figure 8 Effect of the demulsifier concentration (ppm) on the demulsification efficiency for BCH (45) demulsifier at 30% water content and 60 °C.

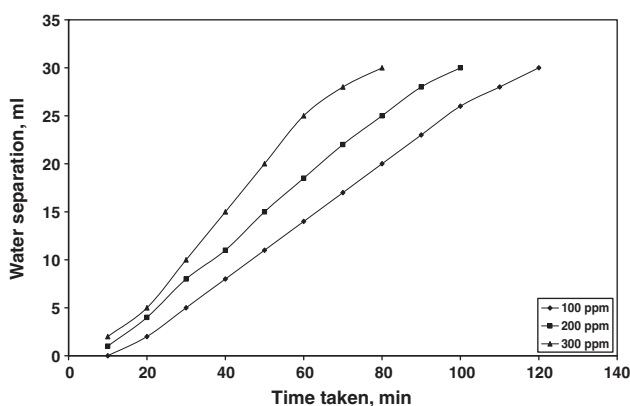


Figure 6 Effect of the demulsifier concentration (ppm) on the demulsification efficiency for BA (27) demulsifier at 30% water content and 60 °C.

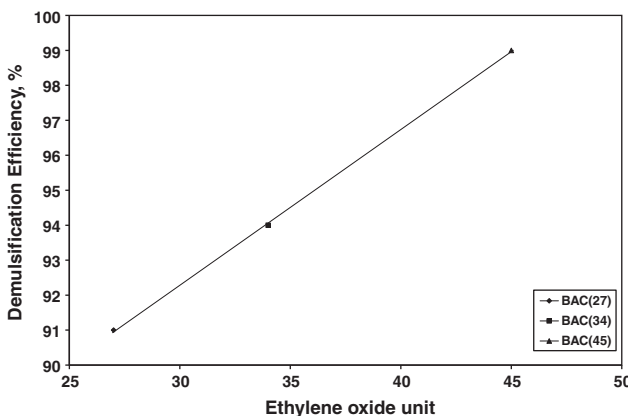


Figure 9 Demulsification efficiency against ethylene oxide unite for BAC (27, 34 and 45) at 30% water content and 100 ppm.

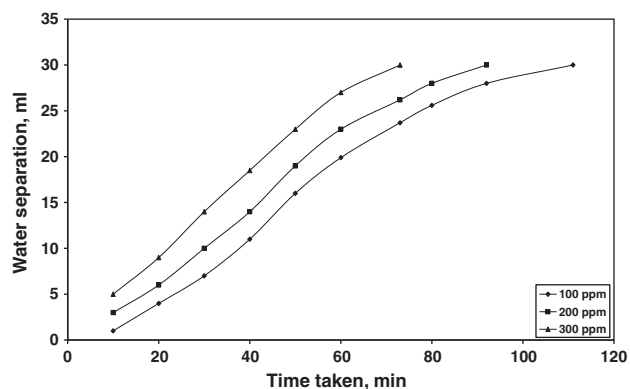
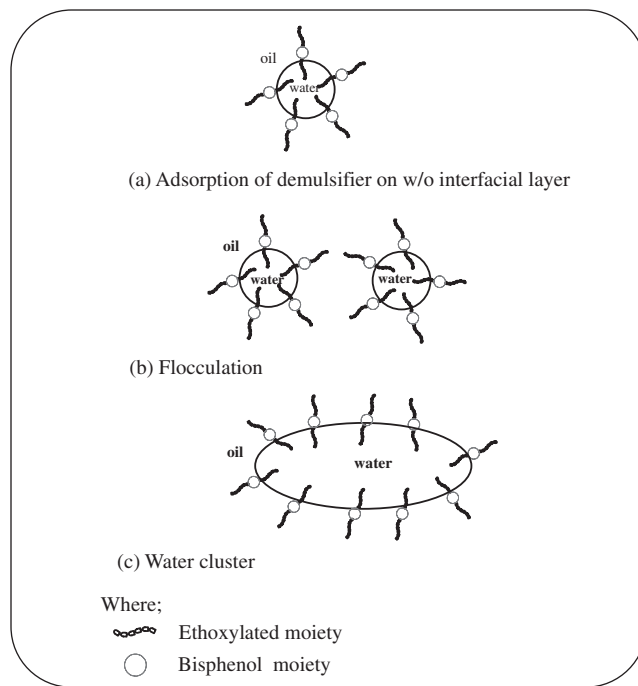


Figure 7 Effect of the demulsifier concentration (ppm) on the demulsification efficiency for BAC (34) demulsifier at 30% water content and 60 °C.

W/O interface, which thus replace the native emulsifiers (asphaltene); this causes the mechanical stability of the interfacial film. The stability of this film continues to decrease and it gets thinner until it collapses totally with further adsorption of the demulsifier agent [20].



Sketch 1 Effect of chemical structure on the mechanism of demulsification efficiency.

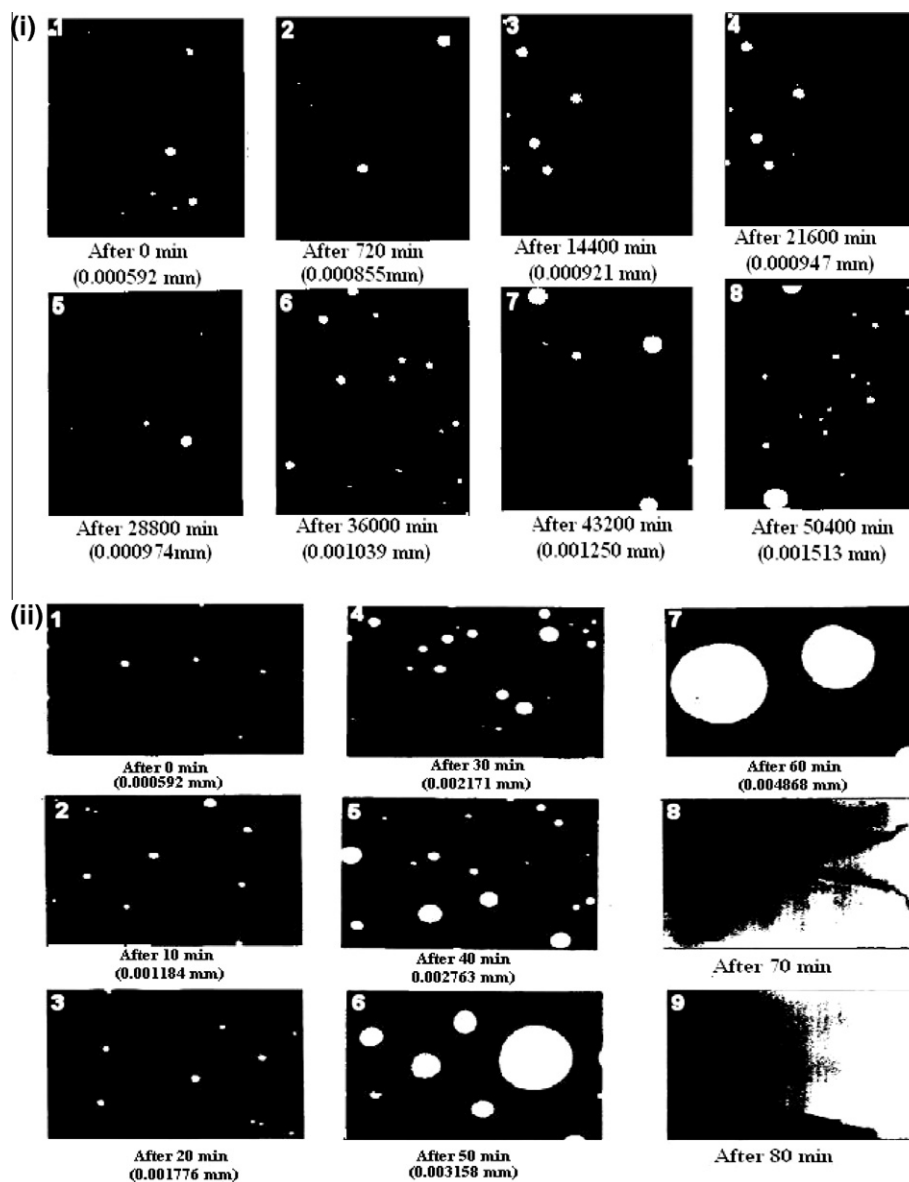


Plate 1 Photographs of: (i) W/O untreated emulsion; (ii) treated emulsion with the BCH (45) as a function of time.

3.3. Chemical structure

3.3.1. Effect of bisphenol structure

Chemical demulsification is an important method of treating W/O emulsions. Amphiphilic structure of demulsifier is divided into a complete hydrophilic moiety (e.o. head) directed toward water droplet and a hydrophobic moiety (bisphenols moiety) directed toward the oil phase. It's of interest to mention that the hydrophilic part of all undertaken demulsifiers in this series contains ethylene oxide chains (EO) with its known hydrophilic character and separated away from the hydrophilic head by different bisphenol skeletons. The variation of such skeleton from completely aliphatic to aliphatic–aromatic or to saturated cyclic affects the leakage of water from water phase into oil phase, which satisfies the hydrophilic tendency of (EO) located in the demulsifier head. It's supposed that the aliphatic–aromatic skeleton of BAC and BCH may hinder the water leakage more than the aliphatic skeleton of BA. This suggestion is based on

the high rigidity and bulkiness of phenyl ring of BAC compared with the methyl side chain of BA. Also, a greater hindrance to water leakage may be exerted by the saturated cyclic cyclohexane of BCH due to its strained and out of plane structure (regarding phenyl plane).

3.3.2. Effect of ethylene oxide content

The effect of the ethoxylated bisphenols (bisphenol A (BA), bisphenol AC (BAC) and bisphenol CH (BCH)) have different units of ethylene oxide ($n = 27, 34, 45$) namely; E (x) demulsifiers, is shown in Tables 2–4 and Fig. 9. Increasing the ethylene oxide content increased the efficiency of demulsifier against all types of the prepared demulsifiers. The time taken for 27 ml water separated (demulsification efficiency = 90%) was 125 min for BAC (27) with ethylene oxide unit (EO) = (27). But the demulsification efficiency against BAC (34) and BAC (45) was 94% and 99%, and the time taken for complete water separation was 111 and 104 min, respectively. This means that

Table 5 Coalescence parameters and coalescence rate constant for untreated and treated emulsion at 30% water content, 300 ppm and 60 °C.

Demulsifier	Time (min)	r (mm) ($\times 10^{-4}$)	$\log(s)$	Rate of coalescence
Control	0*	5.92	3.7047	3.1×10^{-4}
	5*	8.55	3.5450	
	10*	9.21	3.5128	
	15*	9.47	3.5006	3.9×10^{-3}
	20*	9.74	3.4887	
	25*	10.39	3.4603	
	30*	12.50	3.3802	3.6×10^{-3}
	35*	15.13	3.2972	
BAC (45)	0	5.92	3.704722	3.8×10^{-3}
	15	8.03	3.572605	
	30	8.68	3.538391	
	40	13.16	3.357935	1.3×10^{-2}
	50	15.79	3.278754	
	60	37.24	2.906148	2.9×10^{-2}
	71	62.50	2.681241	
BA (45)	0	5.92	3.704722	2.4×10^{-2}
	5	11.84	3.403692	
	10	17.76	3.227601	
	20	21.71	3.140451	3×10^{-2}
	30	27.63	3.035716	
	40	31.58	2.977724	1×10^{-2}
	50	48.68	2.789733	
	58	60.53	2.695177	

* Days instead of minutes.

the maximum surface activity and adsorption capability on the interface of w/o emulsion may be obtained with an ethylene oxide content of 45 units [30]. Accordingly, as the degree of ethoxylation increases, the time required for complete separation decreases. This may be attributed to the molecular average area of absorption at interface which increases with the polyoxyethylene numbers. The molecules of demulsifiers adsorbed at interface loosely. This leads to changing of the film life and interfacial properties [31]. A sketch presenting the orientation of the demulsifier molecules at interface and water leakage is shown in Sketch 1.

3.4. Photography and kinetics of the demulsification process

It is an unfortunate fact that there exists no single coherent theory regarding the mechanism of demulsification. Demulsification is believed to be accompanied by inversion followed by coagulation. It is important to note that the coagulation of the dispersed phase occurs as a two-stage process: flocculation and coalescence. In the second stage, termed coalescence, aggregates combine to form a single drop. This is an irreversible process, leading to a decrease in the number of water droplets and finally to complete demulsification. A third new stage was proposed as a final step in completion of the demulsification process [32]. W/O emulsion photographs for the control and BCH (45) samples as representative examples are shown in Plate 1 as a function of time. From the photographs, one can see that the size of the water droplet increases with time. Table 5 lists the coalescence parameters of the 30% W/O emulsion and also the control sample at 60 °C. The increased water droplet radius leads to an increase in the coalescence rate.

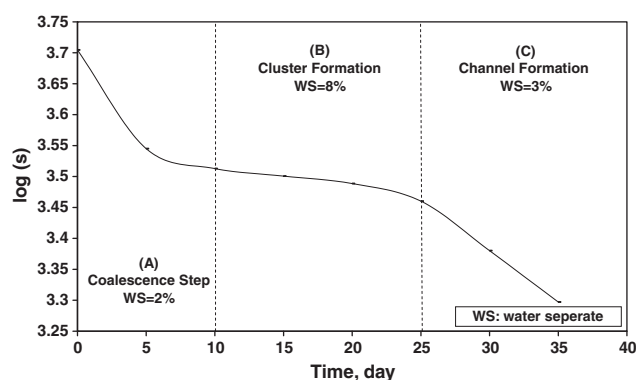


Figure 10 Time taken of demulsification process against $\log(s)$ for control sample with 30% w/o emulsion, 300 ppm and 60 °C.

These data can be analyzed through the plotting of the specific surface area of the water droplet against time, as shown in Figs. 10–12. These plots can be conveniently split into three segments, and each line of the straight segments is described by a first-order rate equation as follows:

$$\log s = -kct \quad (6)$$

where s is the interfacial area per gram of dispersed phase, c is the constant and k is the slope of each line and is measured by the coalescence rate during that period:

$$k = d \log s / dt \quad (7)$$

By analyzing the data in Table 5 and the illustrations in Figs. 10–12, we have found that the demulsification process can be divided into three main steps depending on the demulsification

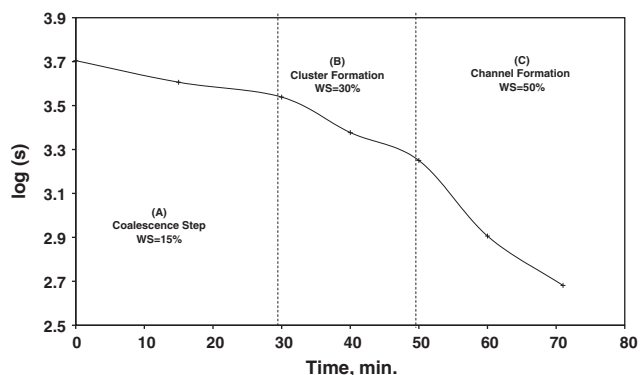


Figure 11 Time taken of demulsification process against $\log(s)$ for BCH (45) at 30% w/o emulsion, 300 ppm and 60 °C.

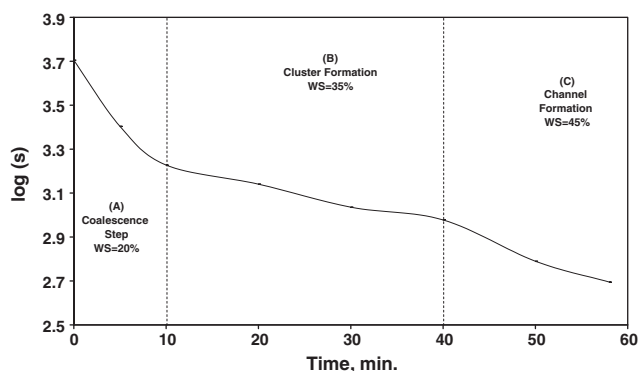


Figure 12 Time taken of demulsification process against $\log(s)$ for BA (45) at 30% w/o emulsion, 300 ppm and 60 °C.

power of the used demulsifier: (A) adsorption and flocculation, in which the demulsifiers adsorb and displace the natural surfactant existing on the W/O interface; (B) cluster formation (coalescence), in which two neighbor water droplets approach each other to form microclusters with low interfacial tension on their W/O interface; and (C) channel formation followed by separation, in which the formed microclusters are collected to form macroclusters and then coagulate to form channels followed by complete water separation. By following the increasing water droplet diameter in Plate 1, it was found that the water droplet size depends on the time of coalescence and the type of demulsifier added. The control sample shows a very slow increase in the water droplet diameter with time: the diameter of the water droplet increases from 5.92 to 9.21×10^{-4} mm after 10 days (step A) and then increases slowly to 10.39×10^{-4} mm after 25 days (step B), at which a water content of 27% is separated. After 35 days, a water content of only 65% is separated. In case of BCH (45) demulsifier, as shown in Fig. 11, the efficiency of

demulsification process increased comparing with untreated sample, whereas, the diameter of water droplet (mm) increases from 5.92 to 62.50×10^{-4} (step C) after 71 min. From the data in Table 5, the rate of coalescence for the control sample was found to be 3.1×10^{-4} , 3.9×10^{-3} and 3.6×10^{-3} for steps A, B, and C, respectively. While, The rate of coalescence of BCH (45) (demulsification efficiency of 99% after 71 min) was 3.8×10^{-3} , 1.3×10^{-2} and 2.9×10^{-2} for the three previous steps (A, B, and C), respectively. However, in the case of BA (45) (demulsification efficiency of 100% after 58 min).

3.5. Surface tension measurements

The data for the surface-active parameters and demulsification efficiency (%) of the prepared demulsifiers are tabulated in Table 6. From the data of demulsification efficiency, it was found that, there is a relation between the surface active properties and the efficiency of demulsifiers. Also, the relation between A_{\min} and the demulsification efficiency is inversely proportional as this means that, the maximum enrichment of the demulsifier molecules on the interface was exhibited with the demulsifier, which has the smallest A_{\min} . At small A_{\min} , the maximum Γ_{\max} should occur and the maximum Γ_{\max} was exhibited with the BA (27), the result of a good demulsification result was obtained. On the other hand, BCH (27) exhibited a lower A_{\min} and higher Γ_{\max} among BA (27) and BAC (27). These results of surface active properties for those demulsifiers consisted of the demulsification efficiency for them. The results of the thermodynamic parameters of adsorption are shown in Table 6 for the same demulsifiers gave evidence on the relation between the surface active proportions and the demulsification efficiency. The more $-\Delta G_{\text{ads}}$ value, indicates that the demulsifier molecules adsorbed strongly on the interface. Generally, the $-\Delta G_{\text{ads}}$ is slightly greater than $-\Delta G_{\text{mic}}$, which means that the molecules prefer to adsorb on the interface than to make micelles. Therefore, the maximum $-\Delta G_{\text{ads}}$ (-27.26 kJ/mol) was obtained with BA (27), which exhibited the maximum demulsification efficiency (time taken for 95% water separation = 120 min at 100 ppm). While the minimum $-\Delta G_{\text{ads}}$ (-24.94 kJ/mol) was obtained with BCH (27), which gave the minimum demulsification efficiency (time taken for 88% water separation = 130 min at the same condition).

References

- [1] L.L. Schramm, Emulsions: Fundamentals and Applications in the Petroleum industry, Adv. Chem. Ser. 231, ACS, Washington DC, 1992.
- [2] D.E. Graham, Crude.Oil. Emulsions, Their Stability and Resolution, Spec. Publ. R. Soc. Chem. (Chem. Oil Ind.) 67 (1988) 155–175.
- [3] E.P. Bourgeois, C. Siffert, B.H. Balard, Fuel 61 (1982) 732–734.

Table 6 Surface tension and thermodynamic properties for some selected demulsifiers at 30% water content, 100 ppm and 25 °C.

Demulsifier	CMC (mol dm ⁻³)	γ_{CMC} (mN/m)	$\Gamma_{\max} \times 10^{10}$ (mol/cm ⁻²)	A_{\min} (nm ²)	π (mN/m)	ΔG_{mic} (kJ/mol)	ΔG_{ads} (kJ/mol)	Demulsifier efficiency (%)
BA (27)	2.01×10^{-5}	31.6	8.59	19.3	40.7	-26.79	-27.26	95
BAC (27)	5.94×10^{-5}	34.3	4.82	34.4	38.0	-24.11	-24.89	90
BCH (27)	6.09×10^{-5}	36.1	4.08	40.6	36.5	-24.05	-24.94	88

- [4] A.L. Bridié, Th.H. Wanders, W. Zegveld, H.B. Van der Heide, *Mar. Poll. Bull.* 11 (1980) 343–348.
- [5] M.E. Ese, J. Sjöblom, H. Fordedal, O. Urdahl, H.P. Ronningsen, *Colloids and Surfaces A: Physicochemical and Engineering Aspects* 123 (1997) 225–232.
- [6] T.J. Jones, E.L. Neustadter, K.P. Whittingham, *The Journal of Canadian Petroleum Technology* 17 (1978) 100–108.
- [7] J.D. McLean, P.K. Kilpatrick, *J. Colloid Interface Sci.* 189 (1997) 242–253.
- [8] S. Taolei, Z. Yiyang, W. Lu, Z. Sui, P. Bo, M. Li, J. Yu, *Journal of Colloid and Interface Science* 255 (2002) 241–247.
- [9] K. Byoung-Yun, J. Hyuk Moon, S. Tea-Hyun, Y. Seung-Man, K. Jong-Duk, *Separation Science and Technology* 37 (6) (2002) 1307–1320.
- [10] J. Im, O. Kwon, J. Kim, S. Lee, *Macromolecules* 33 (26) (2000) 9606–9611.
- [11] J. Wu, Y. Xu, T. Dabros, H. Hamza, *Colloids and Surfaces A: Physicochem Eng. Aspects* 252 (2005) 79–85.
- [12] A.M. Al-Sabagh, M.R. Noor El-Din, R.E. Morsi, M.Z. Elsabee, *Journal of Applied Polymer Science* 108 (2008) 2301–2311.
- [13] J. Djuve, X. Yang, I.J. Fjellanger, J. Sjoblom, E. Pelizzetti, *Colloid Polym. Sci.* 279 (2001) 232–239.
- [14] D. Daniel-David, I. Pezron, C. Dalmazzone, C. Noik, C. Dani'ele, L. Komunjer, *Colloids and Surfaces A: Physicochem. Eng. Aspects* 270–271 (2005) 257–262.
- [15] S.L. Mason, K. May, S. Hartland, *Colloids and Surfaces A: Physicochemical and Engineering* 96 (1995) 85–92.
- [16] A.M. Al-Sabagh, A.M. Badawi, M.R. Noor El-Din, *Petroleum Science and Technology* 20 (2002) 887–914.
- [17] H. Abdurahman, R.Y. Nour, Z. Jemaat, *J. of Applied Science* 7 (2) (2007) 196–201.
- [18] A. AL-Sabagh, M. Nermine, E. Maysour, M.R. Noor El-Din, *Journal of Dispersion Science and Technology* 28 (2007) 547–555.
- [19] M.J. Rosen, S. Aronson, *Colloids Surf A: Physicochemical and Engineering* 3 (1981) 201–208.
- [20] A.M. Al-Sabagh, M.E. Abdul-Raouf, R. Abdel-Raheem, *Colloids Surf A: Physicochemical and Engineering* 251 (2004) 167.
- [21] A.M. Al-Sabagh, *Polym. Adv. Technol.* 11 (2000) 48.
- [22] M.J. Rosen, *Surfactants and Interfacial Phenomena*, Wiley, New York, 1978.
- [23] C. Wu, J.L. Zhang, W. Li, N. Wu, *Fuel* 84 (2005) 2093.
- [24] L.L. Schramm, *Surfactants: Fundamentals and Applications in Petroleum Industry*, Cambridge University Press, Cambridge, England, 2000.
- [25] C.S. Shetty, A.D. Nikolov, D.T. Wasan, *J. Dispersion Sci. Technol.* 13 (1992) 121.
- [26] M.J. Rosen, S. Aronson, *Colloids Surf. A: Physicochemical and Engineering* 3 (1981) 201.
- [27] J.W. Gibbs, *Longman* 1 (1928) 119.
- [28] A. Bharadwaj, S. Hartland, *Ind Eng Chem Res* 33 (1994) 1271.
- [29] A.M. Al-Sabagh, M.R. Noor El-Din, S. Abo-El Fotouh, N.M. Nasser, *Journal of Dispersion Science and Technology* 30 (2009) 267–276.
- [30] A.K. Mark, T.W. Darsh, S.S. Chandashekar, *Ind. Eng. Chem. Res.* 30 (8) (1991) 1997.
- [31] W. Kanga, G. Jing, H. Zhang, M. Li, Z. Wu, *Colloids and Surfaces A: Physicochem Eng. Aspects* 272 (2006) 27–31.
- [32] H.K. Young, T.W. Drash, *Ind. Eng. Chem. Res.* 35 (1996) 1141–1149.